Sensitivity analysis of DEM prediction for sliding wear by single iron ore particle

Chen, Guangming; Schott, Dingena; Lodewijks, Gabri

DOI
10.1108/EC-07-2016-0265

Publication date
2017

Document Version
Final published version

Published in
Engineering Computations: international journal for computer-aided engineering and software

Sensitivity analysis of DEM prediction for sliding wear by single iron ore particle

Guangming Chen, Dingena L. Schott and Gabriel Lodewijks
Department of Maritime and Transport Technology, Delft University of Technology, Delft, The Netherlands

Received 23 July 2016
Revised 5 January 2017
Accepted 28 March 2017

Abstract

Purpose – Sliding wear is a common phenomenon in the iron ore handling industry. Large-scale handling of iron ore bulk-solids causes a high amount of volume loss from the surfaces of bulk-solids-handling equipment. Predicting the sliding wear volume from equipment surfaces is beneficial for efficient maintenance of worn equipment. Recently, the discrete element method (DEM) simulations have been utilised to predict the wear by bulk-solids. However, the sensitivity of wear prediction subjected to DEM parameters has not been systemically investigated at single particle level. To ensure the wear predictions by DEM are accurate and stable, this study aims to conduct the sensitivity analysis at the single particle level.

Design/methodology/approach – In this research, pin-on-disc wear tests are modelled to predict the sliding wear by individual iron ore particles. The Hertz–Mindlin (no slip) contact model is implemented to simulate interactions between particle (pin) and geometry (disc). To quantify the wear from geometry surface, a sliding wear equation derived from Archard's wear model is adopted in the DEM simulations. The accuracy of the pin-on-disc wear test simulation is assessed by comparing the predicted wear volume with that of the theoretical calculation. The stability is evaluated by repetitive tests of a reference case. At the steady-state wear, the sensitivity analysis is done by predicting sliding wear volumes using the parameter values determined by iron ore-handling conditions. This research is carried out using the software EDEM® 2.7.1.

Findings – Numerical errors occur when a particle passes a joint side of geometry meshes. However, this influence is negligible compared to total wear volume of a wear revolution. A reference case study demonstrates that accurate and stable results of sliding wear volume can be achieved. For the sliding wear at steady state, increasing particle density or radius causes more wear, whereas, by contrast, particle Poisson's ratio, particle shear modulus, geometry mesh size, rotating speed, coefficient of restitution and time step have no impact on wear volume. As expected, increasing indentation force results in a proportional increase. For maintaining wear characteristic and reducing simulation time, the geometry mesh size is recommended. To further reduce simulation time, it is inappropriate using lower particle shear modulus. However, the maximum time step can be increased to 187% T_R without compromising simulation accuracy.

Research limitations/implications – The applied coefficient of sliding wear is determined based on theoretical and experimental studies of a spherical head of iron ore particle. To predict realistic volume loss in the iron ore-handling industry, this coefficient should be experimentally determined by taking into account the non-spherical shapes of iron ore particles.

Practical implications – The effects of DEM parameters on sliding wear are revealed, enabling the selections of adequate values to predict sliding wear in the iron ore-handling industry.

Originality/value – The accuracy and stability to predict sliding wear by using EDEM® 2.7.1 are verified. Besides, this research accelerates the calibration of sliding wear prediction by DEM.

Keywords Discrete element method, Pin-on-disc, Bulk-solids-handling, Wear prediction

Paper type Research paper

The authors are grateful to China Scholarship Council-CSC (No. 201206170158) for funding this research.

Engineering Computations
Vol. 34 No. 6, 2017
pp. 2031-2053

0264-4401
DOI 10.1108/EC-07-2016-0265

Nomenclature

Latin

a = Radius of indentation area by a spherical particle [m]
A_0 = Area of cross section by spherical particle indentation [m^2]
A_N = Real loss of area from displace groove for N revolutions [m^2]
A_r = Real loss of area from displace groove for one revolution [m^2]
C = Damping coefficients [$(N{\cdot}kg/m)^{1/2}$]
d_0 = Mesh size [m]
e = Restitution between particle and geometry mesh [dimensionless]
E = Young's modulus [GPa]
F = Force [N]
G = Shear modulus [GPa]
H_e = Hardness of equipment surface [GPa]
l = Sliding distance [m]
m = Mass [kg]
N = Number of revolutions [dimensionless]
P_m = Maximum pressure stress by a spherical particle [Pa]
r_0 = Distance between pin and disc central axis [m]
R = Radius [m]
S = Spring stiffness [N/m]
Δt = Time step [s]
T = Time [s]
T_R = Rayleigh time [s]
v = Velocity [m/s]
W_V = Wear volume [m^3]

Greek

α = Sliding wear coefficient [m^2/N]
β = Coefficient that relates to restitution [dimensionless]
δ = Overlap [m]
ϕ = Coefficient of fraction [dimensionless]
λ = A factor used to calculate particle shear modulus [dimensionless]
μ = Coefficient of friction between particle and mesh [dimensionless]
ν = Poisson's ratio [dimensionless]
θ = Angle of the indentation curvature [radian]
ρ = Density [kg/m^3]
σ_c = Yield stress [Pa]

Indices

d = Disc
g = Geometry
h = Holder
n = Normal
p = Particle
s = Sliding
t = Tangential
$*$ = Equivalent

1. Introduction

The sliding wear by particles is caused by the relative sliding motions between particles and equipment surfaces. In bulk-solids-handling, sliding wear is a common phenomenon which occurs for instance, on the surface of transfer chute bottoms (Roberts, 2003). Iron ore (Miszewski *et al.*, 2012; Lommen, 2016) is a type of bulk-solid and is used as raw material for steel products. Owing to economic developments, iron ore mining remains intensive, which promotes a large-scale iron ore-handling industry. Natural iron ore particles have high hardness, irregular shapes and various sizes [from microns to centimetres (Miszewski *et al.*, 2012; Lommen, 2016)]; thus, a high amount of sliding wear volume occurs to the surfaces of bulk-solids-handling equipment. The sliding wear accelerates the damage of bulk-solids-handling equipment and increases downtime. To efficiently maintain worn equipment, a numerical simulation method to predict sliding wear can be used.

The discrete element method (DEM) (Cundall and Strack, 1979) is an important numerical technique which can be used to simulate the behaviours of particulate systems (Mishra and Rajamani, 1992) and examine effects of parameters (Keppler *et al.*, 2016a; 2016b). Wear can be predicted by implementing wear equations in the DEM simulations (Rezaeizadeh *et al.*, 2010; Powell *et al.*, 2011; Jafari and Nezhad, 2016). In bulk-solids-handling industry, the wear by particle collision and abrasion has been explored by DEM with respect to several pieces of bulk-solids-handling equipment. These items are mill liners (Cleary, 1998; Kalala and Moys, 2004; Cleary *et al.*, 2010; Powell *et al.*, 2011), mill lifters (Cleary *et al.*, 2006; Rezaeizadeh *et al.*, 2010), mill discs (Sato *et al.*, 2010), screen mesh (Cleary *et al.*, 2009; Jafari and Nezhad, 2016), piping wall (Tan *et al.*, 2012) and transfer chutes (Xie *et al.*, 2016).

These wear predictions from the DEM simulations have shown promising results and all focus on sets of particles assuming that the wear prediction by a single particle is correctly established. However, to obtain the sum of wear volume from geometry meshes (Powell *et al.*, 2011), several parameters affect the contact between particles and meshes and therefore this should be carefully investigated. For instance, Jourani and Bouvier (2015) concluded that particle size (radius) might affect sliding wear, and Powell *et al.* (2011) suggested evaluation of the effects of mesh sizes on the wear predictions. Nevertheless, at single particle levels, the sensitivity analysis of the sliding wear prediction by the DEM parameters has not yet been studied in detail by the research community.

This research presents the sensitivity analysis of DEM parameters on the sliding wear predictions based on the modelled pin-on-disc tests using the software EDEM® 2.7.1 (DEM Solutions, 2016). Based on Archard's wear model, a sliding wear equation is derived and is implemented in the DEM simulations. After verification of this simulation model, the sliding wear with regard to DEM parameters are obtained.

The organisation of this paper is as follows:

- Section 2: Illustrates the methodology of simulating sliding wear.
- Section 3: Presents the determinations of DEM parameters.
- Section 4: Analyses the reference case of sliding wear prediction.
- Section 5: Provides the sensitivity study of DEM parameters.
- Section 6: Draws the conclusions of this research.

2. Methodology

To model the sliding wear by iron ore particles by DEM, this section presents the methodology of predicting the sliding wear for a single particle in a pin-on-disc simulation model. It also includes the implemented sliding wear equation to quantify wear volume. The

simulation model has the identical scale as our laboratory setup and is built in EDEM® 2.7.1 (DEM Solutions, 2016). The pin-on-disc wear test is conducted based on the standard test method (ASTM, 2000).

2.1 Sliding wear equation

Figure 1(a) illustrates the three-dimensional sliding wear model using a spherical particle and a flat surface of ductile material. In Figure 1(a), v_t is the relative sliding velocity of the particle; F_p is the indentation force; and l is the sliding distance. However, in the DEM simulations, a geometry surface is constructed with meshes which interact with particles. Figure 1(b) shows the two-dimensional sliding wear models with respect to both a continuous and a meshed surface. In Figure 1(b), F_n is the reaction force from geometry surface caused by particle indentation and d_0 is the mesh size. The implemented sliding wear equation is illustrated as follows.

Based on Archard's wear model (Archard, 1953), the wear volume W_V for the sliding wear model as in Figure 1(a) is estimated by:

$$W_V = \alpha_s \cdot F_n \cdot l \tag{1}$$

where α_s is the coefficient of sliding wear. Referring to equation (1) and Figure 1(b), the sliding wear from a meshed geometry surface for a distance l is given by:

$$W_V = \alpha_s \cdot F_n \cdot \sum d_0 = \alpha_s \cdot F_n \cdot v_t \cdot T \tag{2}$$

where v_t is relative tangential velocity and Δt is time step. For the reaction force F_n, it can be expressed as the resultant force of a Hertz normal force (Popov, 2010) and a normal damping force (Barrios *et al.*, 2013), which is:

$$F_n = -K_n \delta_n + C_n v_n \tag{3}$$

where K_n is normal stiffness; δ_n is normal overlap; C_n is the coefficient for normal damping force; and v_n is indentation velocity. The expressions for K_n and C_n are given in Tables I and II. By inserting equations (3) to (2), the prediction of total wear volume W_V is:

$$W_V = \alpha_s \cdot (-K_n \delta_n + C_n v_n) \cdot v_t \cdot T \tag{4}$$

The frictional force (F_t) between particle and geometry is restrained by Coulomb law, which is:

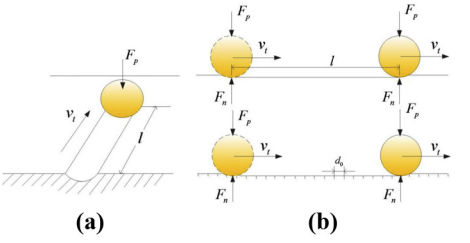

Notes: (a) 3D schematic for a flat surface; (b) 2D illustration for a flat surface and a meshed surface

Figure 1.
Sliding wear model

$$F_t = \min\{\mu F_n, -S_t\delta_t + C_t v_t\} \quad (5)$$

where S_t and C_t are, respectively, tangential stiffness and coefficient for tangential damping force. The expressions for S_t and C_t are also provided in Table I. The equivalents and the related expressions are given in Table II. All the used symbols are listed in the Nomenclature.

2.2 Simulation model

Figure 2 shows the simulation model of a pin-on-disc wear test which is built using the software EDEM® 2.7.1 (DEM Solutions, 2016). Here ω is the angular velocity of the disc geometry with respect to its central axis (OO') and F_p is the indentation force acting on the pin particle. The meshed disc geometry has a radius of 0.0265 m and a height of 0.006 m, which is used as the model of the mild steel disc. A single mono-size spherical particle is used to represent Sishen iron ore (Kano *et al.*, 2005). This particle is positioned at a distance r_O = 0.022 m with regard to the central axis OO' and thus a full revolution is 0.1382 m. To restrain the particle movements incurred by the rotating disc, a holder is applied and the rolling motion of the particle is disabled. The central axis of the holder is parallel to that of the disc and goes through the contact point between particle and geometry. To generate a

Coefficients	Normal direction	Tangential direction
Spring stiffness	$S_n = 2E^*\sqrt{R^*\delta_n}$	$S_t = 8G^*\sqrt{R^*\delta_n}$
Damping	$C_n = 2\sqrt{\frac{5}{6}}\beta\sqrt{S_n m^*}$	$C_t = 2\sqrt{\frac{5}{6}}\beta\sqrt{S_t m^*}$

Source: Powell *et al.* (2011)

Table I. Coefficients of spring stiffness and damping in normal and tangential directions

Equivalents	$\frac{1}{E^*} = \frac{1-v_p}{2G_p} + \frac{1-v_g}{2G_g}$	$\frac{1}{G^*} = \frac{2-v_p}{G_p} + \frac{2-v_g}{G_g}$
	$\frac{1}{R^*} = \frac{1}{R_p} + \frac{1}{R_g}$	$\frac{1}{m^*} = \frac{1}{m_p} + \frac{1}{m_g}$
Other expressions	$\beta = \frac{-\ln e}{\sqrt{\ln^2 e + \pi^2}}$	$K_n = \frac{4}{3}E^*\sqrt{R^*\delta_n}$

Source: Powell *et al.* (2011)

Table II. Equivalents and other expressions

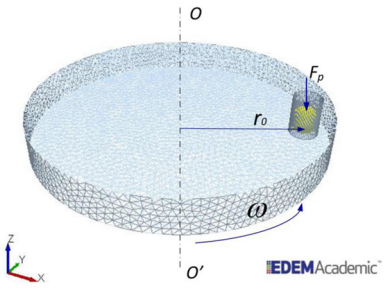

Figure 2. Pin-on-disc simulation model

particle in the holder, the radius of holder has to be slightly larger than the radius of the modelled particle. Herein, the radius of the holder is set 0.0001 m larger than the particle.

Figure 3 illustrates the DEM simulation cycle of modelling a pin-on-disc wear test. It implies that, as geometry rotates, the simulation model subsequently undergoes four procedures in each time step until the simulation time has been reached. These four procedures are: apply indentation force, detect contact, calculate wear and update contact. The indentation force on particle is applied by the particle body force of EDEM® API (DEM Solutions, 2016) and the global gravitational force. The Hertz–Mindlin no-slip contact model (Barrios *et al.*, 2013) is used to calculate the contact forces between particle and geometry. The wear volume from geometry surface is obtained by the implemented sliding wear equation (4).

Thus far, the sliding wear equation and the DEM cycle for modelling a pin-on-disc wear test have been illustrated. Using this simulation model and appropriate input values of DEM parameters, the sliding wear by iron ore particle can be predicted. In the following section, the determination of the DEM parameter values for modelling the pin-on-disc wear test is presented.

3. Determination of DEM parameter values

This section determines the DEM parameter values to predict sliding wear by using the simulation model of pin-on-disc wear test. All the DEM parameters are classified into four categories, namely, particle, geometry, contact and simulation. In this research, the values of the DEM parameters are determined on the basis of available resources and our current experimental wear tests.

3.1 Particle parameters

From the sliding wear equation (4) and the entailed parameters in Table I, four particle parameters require to be determined, which are:

(1) radius R_p;

(2) density ρ_p;

(3) Poisson's ratio ν_p; and

(4) shear modulus G_p.

The determination of these four particle parameters is shown as follows:

A sample of the used particles of Sishen iron ore is shown in Figure 4(a). Referring to its particle size distribution in Figure 4(b) and the median size d_{50} = 3 mm (Miszewski *et al.*, 2012; Lommen, 2016), the modelled spherical particles radii can be 1-4 mm to account for the

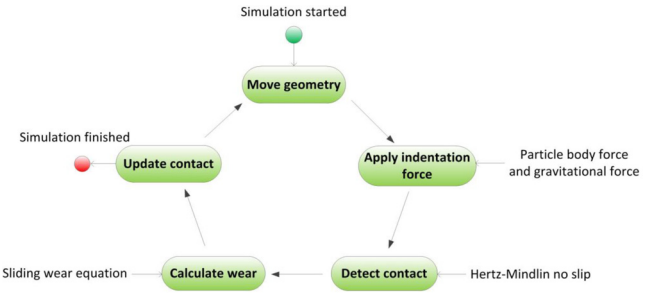

Figure 3.
Simulation cycle of a pin-on-disc wear test

Source: DEM Solutions (2016)

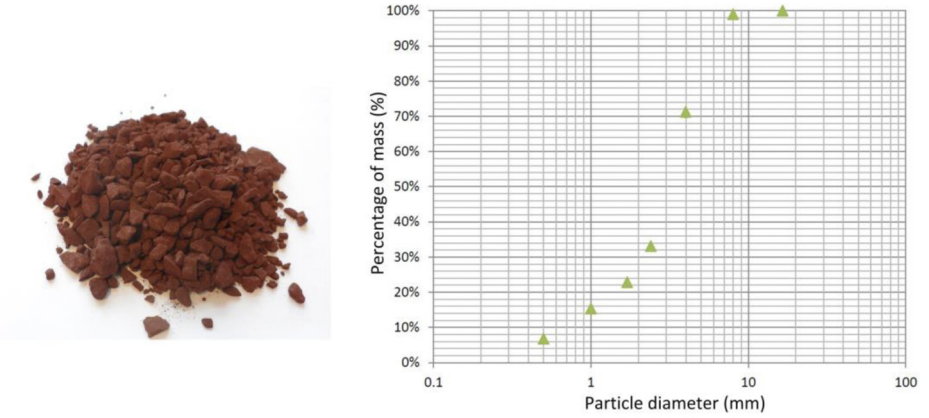

(a) (b)

Figure 4. Sishen iron ore sample

Notes: (a) Referred sample; (b) the particle size distribution

sizes of majority particles. Using a gas-expansion pycnometer, we measure that particle densities extend from 4,768 to 4,970 kg/m^3 for small and big sizes, and the average density is 4,865 kg/m^3.

Because Sishen iron ore contains a large percentage of hematite (Taylor *et al.*, 1988), the Poisson ratio is comparable to 0.24 according to available experimental research by Minoru and Yasuo (1983). In combination with the variances of particle densities and inner micro-structures, the Poisson ratio of Sishen iron ore is estimated in the range of 0.23-0.26. The shear modulus of Sishen particles is determined according to George (1961):

$$G = \frac{E}{2(1+\nu)} \tag{6}$$

In equation (6), the Young's modulus of iron ore particle is calculated based on an empirical formula (Minoru and Yasuo, 1983), which is expressed by:

$$E_p = 55.27 + 128.87\left(\rho_p/1000 - 4.0\right) \tag{7}$$

Using equation (7) and the measured Sishen particle densities ρ_p = (4,768-4,970) kg/m^3, the Young's modulus of iron ore particle is calculated at (154.24-180.27) GPa. Using the result of the calculated Young's modulus and the average value of the particle Poisson's ratio 0.24, the shear modulus is determined at (62.19-72.69) GPa by applying equation (6).

Table III summarises the determined values for the particle parameters.

Category	DEM parameters	Values
Particle	Radius R_p [$\times 10^{-3}$ m]	1-4
	Density ρ_p [kg/m^3]	4,768-4,970
	Poisson's ratio v_p	0.23-0.26
	Shear modulus G_p [GPa]	62.19-72.69

Table III. Values for particle parameters

3.2 Geometry parameters

Based on the geometry parameters in equation (4), and the related parameters in Tables I and II, while also accounting for geometry mesh size, totally five geometry parameters need to be determined:

(1) density ρ_g;
(2) Poisson's ratio v_g;
(3) shear modulus G_g;
(4) rotating speed ω; and
(5) mesh size d_0.

The determinations of the geometry parameters for the disc and holder are presented as follows.

For the disc that is modelled as mild steel, its density is measured as 7,930 kg/m^3. The Poisson's ratio and shear modulus of mild steel refer to in available research (Brown *et al.*, 2014) as 0.3 and 78 GPa, respectively. For maintaining consistency with our laboratory pin-on-disc wear test, we set the rotating speeds of the disc as (2.27-15.91) rad/s, resulting in sliding velocity 0.05-0.35 m/s. A higher velocity than 0.35 m/s causes undesirable vibrations for our laboratory pin-on-disc tests. The geometry is meshed into tetrahedrons using the software ANSYS® 16.2 (ANSYS, 2016). To achieve smooth transition between the triangle meshes, the maximum size of mesh sides is set by 4.4×10^{-3} m. By accounting for the reduction of computational time that is proportional to the number of meshes, the minimal size is set by 0.55×10^{-3} m.

Table IV presents the determined values for the disc geometry parameters.

The geometry parameters of cylindrical holder do not influence the steady-state wear. Therefore, a standard cylindrical geometry in the software EDEM® 2.7.1 (DEM Solutions, 2016) is used to create the holder. Furthermore, the default values are applied as inputs to the geometry parameters.

Table V lists the values used for holder geometry parameters.

3.3 Contact parameters

Referring Tables I and II, three parameters are involved as the contact parameters for the interactions between particle and geometries of disc and holder, which are:

Table IV.
Values for the disc geometry parameters

Item	DEM parameters	Values
Disc	Density ρ_g [kg/m^3]	7,932
	Poisson's ratio v_g	0.3
	Shear modulus G_g [GPa]	78
	Rotating speed ω [rad/s]	2.27-15.91
	Mesh size d_0 [$\times 10^{-3}$m]	0.55-4.4

Table V.
Values for the holder geometry parameters

Item	DEM parameters	Values
Holder	Density ρ_h [kg/m^3]	2,500
	Poisson's ratio v_h	0.25
	Shear modulus G_h [GPa]	0.1

- coefficient of restitution e;
- coefficient of static friction μ_s; and
- coefficient of rolling friction μ_r.

The values for these three parameters for disc and holder are determined in the following manner.

For the contact between particle and disc, the coefficient of restitution refers to experimental tests of iron ore pellets (Barrios *et al.*, 2013), which is 0.42. By accounting for the variety of the shape and densities of Sishen iron ore particles, a range of 0.35-0.50 is applied to the coefficient of restitution. According to equation (4), the wear volume is not related to the coefficient of friction. Therefore, the value of 1.0 is applied to the coefficient of friction to minimise particle sliding movement before reaching a steady-state wear. Even though the particle is not allowed to roll, the coefficient of rolling friction is given by zero according to Brown *et al.* (2014).

Table VI provides the determined values for the contact between particle and disc geometry.

For the interaction between particle and holder, the value of coefficient of restitution is significantly low so that the response of the particle during the contact with the holder is largely damped. The other inputs of coefficients of static friction and rolling friction are identical to those of particle/disc contact.

Table VII gives the values for the contact between particle and holder.

3.4 Simulation parameters

According to equation (4), and also accounting for time step, the following four simulation parameters are required to predict the wear by the DEM simulation model:

(1) indentation force F_p;

(2) coefficient of sliding wear α_s;

(3) sliding distance l; and

(4) time step Δt.

The determination of the values for these four parameters are shown as follows.

First, a range of 3-9 N is utilised for indentation force in accordance with the estimations of the contact pressure between particle and equipment under bulk-solids-handling

Table VI. Values for the contact parameters between particle and disc

Category	DEM parameters	Values
Particle/Disc contact	Coefficient of restitution $e_{p,d}$	0.35-0.50
	Coefficient of static friction $\mu_{s,p,d}$	1.0
	Coefficient of rolling friction $\mu_{r,p,d}$	0

Table VII. Values for the contact parameters between particle and holder

Category	DEM parameters	Values
Particle/Holder contact	Coefficient of restitution $e_{p,h}$	0.0001
	Coefficient of static friction $\mu_{s,p,h}$	1.0
	Coefficient of rolling friction $\mu_{r,p,h}$	0

conditions (Roberts and Wiche, 1993). To determine the coefficient of sliding wear α_s, Figure 5 illustrates the indentation characteristic for a sphere indenting a ductile flat surface, in which δ_n is the normal overlap; A_O is the curved area of the cross-section of indentation; θ is the angle of the indentation curvature; and a is the circle radius for the contact area. α_s is determined by equation (8) and its derivation is given in Appendix 1:

$$\alpha_s = \frac{3\phi\left[arc\sin\left(\frac{\delta_n}{R_p}\right)^{1/2} - \left(\frac{\delta_n}{R_p}\right)^{1/2} + \left(\frac{\delta_n}{R_p}\right)^{3/2}\right]}{4E^*\left(\frac{\delta_n}{R_p}\right)^{3/2}} \tag{8}$$

In equation (8), $\frac{\delta_n}{R_p}$ is suggested as a constant for a given applied load regardless of particle sizes (Bingley and Schnee, 2005). $\frac{\delta_n}{R_p}$ is estimated at 5.58×10^{-5} referring to Appendix 2. ϕ is the fraction of material removal from the displaced groove area A_O. A laboratory test is executed using a spherical head of an iron ore particle sliding against a mild steel surface; this results in $\phi = 0.84$ (illustrated in Appendix 3). E^* is estimated at 96.74 GPa by using its expression in Table I. Eventually, equation (8) gives $\alpha_s = 6.51 \times 10^{-12}$ m^2/N. The sliding distance is set to 180 m (corresponding to 20 min) for conveniently measuring wear loss, which refers to our laboratory pin-on-disc tests. The last simulation parameter of time step is estimated using the Rayleigh time step that is:

$$T_R = \pi R_p \sqrt{\rho_p / G_p} / (0.1631 P_p + 0.8766) \tag{9}$$

In DEM simulations, a lower value than Rayleigh time step is commonly used for increasing the accuracy of the simulation results. However, in attempting to reduce computational time and maintain simulation accuracy, the test range of values for time step $\Delta t = (50\text{-}130)\% T_R$.

Table VIII lists the determined values for the simulation parameters.

4. Reference case

Section 3 presents the determined values of the DEM parameters for wear predictions. By selecting the determined values as inputs, this section will verify the accuracy and the stability of the simulation model.

From Tables III-VIII, a group of values used as a reference case is selected, which is given in Table IX. Correspondingly, Figure 6 presents the wear prediction, in which the legend bar

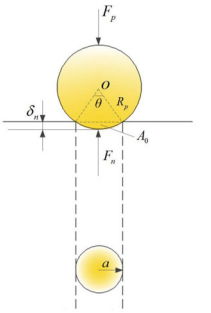

Figure 5.
Rigid spherical particle indents against an elastic surface

Source: Popov (2010)

represents the magnitude of the wear volume from each mesh. Owing to the nonuniform meshes, the wear volumes from each worn mesh are inequivalent.

To verify the accuracy of the predicted wear volume, Figure 7 presents the result of the reaction force in accordance with each time step for the early wear stage. This figure shows that the reaction force (F_n) initially increases to maximum, then it decreases with fluctuations and finally arrives at an expected constant. These overshoots are caused by the variance of overlap when applying the external force, i.e. particle body force. The predicted forces are consistent with the theory of equation (3). Moreover, this figure shows that the reaction force reaches its steady value at a very short time.

Figure 8 presents the particle tangential velocity corresponding to the early wear stage. Initially, the tangential velocity exhibits similar characteristics as that of the reaction force until it reaches a constant value. However, it begins to decrease when the particle comes in contact with the holder surface. From the moment 0.0012 s onwards, the particle tangential velocity becomes zero, which means that the movement of particle has been restrained.

It is expected that the particle tangential velocity maintains a constant of zero after 0.0012 s. However, the particle tangential velocity overshoots intermittently and triggers occurrences of numerical errors, as presented in Figure 9.

Table VIII. Values for the simulation parameters

Category	DEM parameters	Values
Simulation	Indentation force F_p [N]	3-9
	Coefficient of sliding wear α_s [$\times 10^{-12}$ m^2/N]	6.51
	Sliding distance l [m]	180
	Time step Δt [$\times 10^{-6}$ s]	1.0-2.5

Table IX. Reference case of determined DEM parameter values for pin-on-disc wear test

Categories	Items	DEM parameters	Values
Particle	Iron ore	Radius R_p [$\times 10^{-3}$ m]	2
		Density ρ_p [kg/m^3]v	4,850
		Poisson's ratio ν_p	0.24
		Shear modulus G_p [GPa]	65
Geometry	Disc	Density ρ_d [kg/m^3]	7,932
		Poisson's ratio ν_d	0.3
		Shear modulus G_d [GPa]	78
		Rotating speed ω [rad/s]	6.82
		Mesh size d_O [$\times 10^{-3}$m]	1.1
	Holder	Density ρ_h [kg/m^3]	2,500
		Poisson's ratio ν_h	0.25
		Shear modulus G_h [GPa]	0.1
Contact	Iron ore/disc	Coefficient of restitution $e_{p,d}$	0.4
		Coefficient of static friction $\mu_{s,p,d}$	1.0
		Coefficient of rolling friction $\mu_{r,p,d}$	0
	Iron ore/holder	Coefficient of restitution $e_{p,h}$	0.0001
		Coefficient of static friction $\mu_{s,p,h}$	1.0
		Coefficient of rolling friction $\mu_{r,p,h}$	0
Simulation	Condition	Indentation force F_p [N]	5
		Coefficient of sliding wear α_s [$\times 10^{-12}$ m^2/N]	6.51
		Sliding distance l [m]	180
		Time step Δt [$\times 10^{-6}$s]	1.5

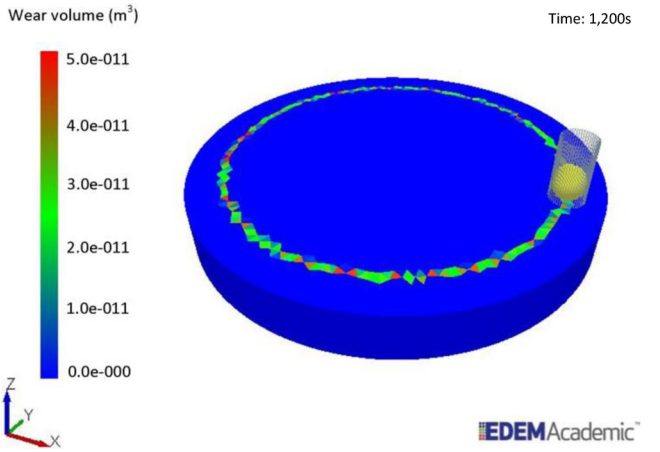

Figure 6.
Wear for a sliding distance of 180 m of the reference case

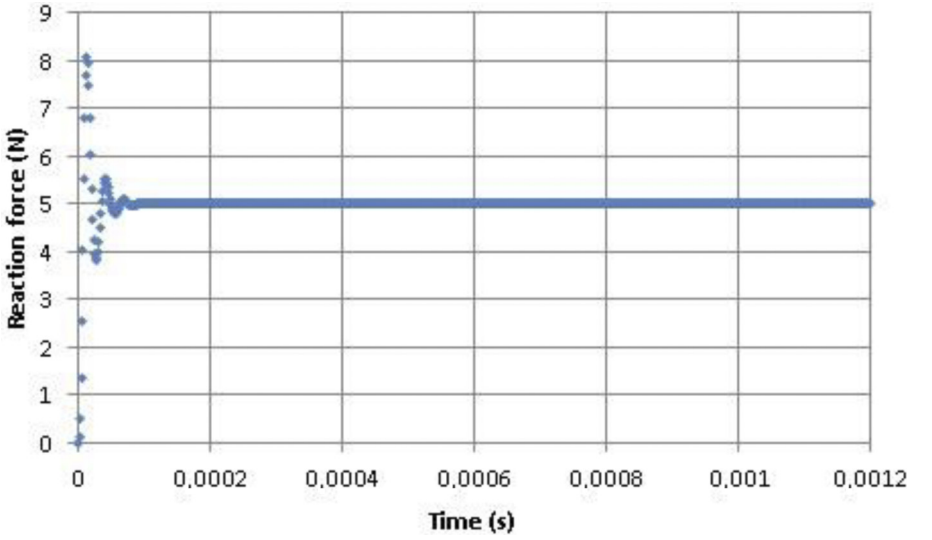

Figure 7.
Reaction force as at an early wear stage

To further analyse the numerical scattered data, the first occurrence in Figure 9 is represented in Figure 10. It shows that particle tangential velocity drops to a negative value but immediately changes to positive. After going up to a peak, the velocity decreases quickly to below zero, then it gradually returns to zero. By comparing the sudden increase with the wear track in Figure 6, it is concluded that a numerical error occurs whilst the particle crosses a joint side of geometry meshes.

To examine the influence of the scattered data on total wear, the wear volume corresponds to the early stage 0.012 s is illustrated in Figure 11. Figure 9 demonstrates that the total wear can maintain a linear increase even when numerical scattered data are incurred. This indicates that the influence of the numerical scattered data is negligible in

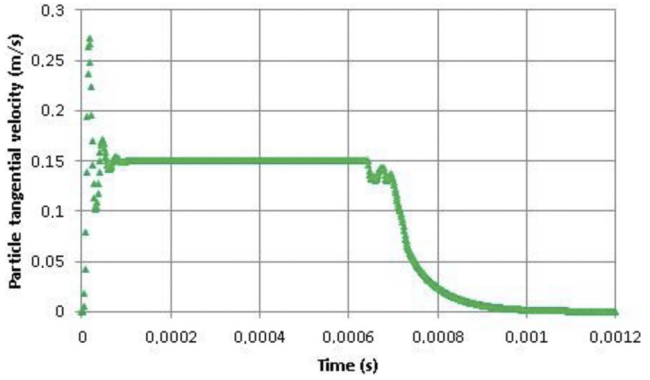

Figure 8.
Particle tangential velocity at an early wear stage

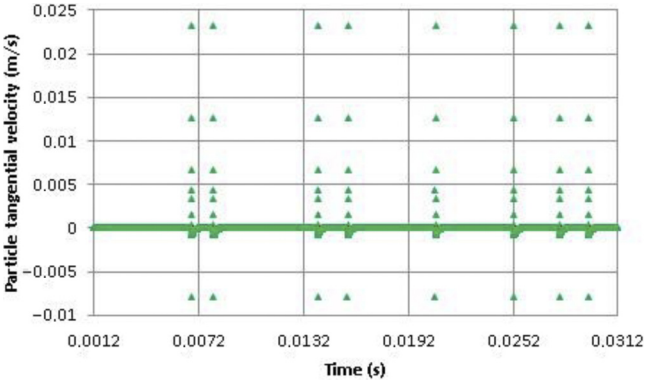

Figure 9.
Particle tangential velocity for fully contact with holder

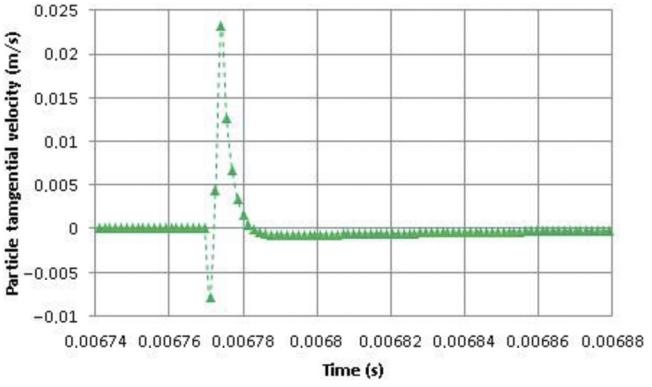

Figure 10.
Identification of numerical scattered data as a particle passes a joint side of meshes

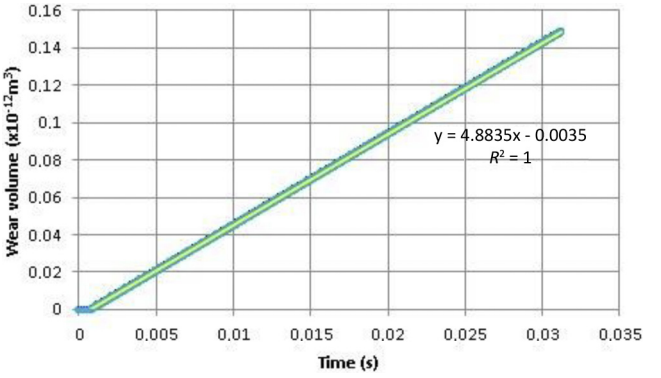

Figure 11.
Wear volume as a function of time at the early stage

comparison with the total wear, especially when considering that sliding distance is in the range of meters. Furthermore, the linear increase of volume indicates that steady-state wear starts after the particle has been fully contacted with holder.

Figure 12 shows the predicted wear volume over the sliding distance of 180 m at the steady state. It is observed that the linear characteristic of wear as that in Figure 11 is maintained. The predicted wear volume is $5{,}861 \times 10^{-12}$ m^3, which differs less than 0.04 per cent with the theoretical calculation of $5{,}859 \times 10^{-12}$ m^3 using equation (4). Thus, accuracy of the DEM prediction of wear is verified.

In addition, stability tests are carried out by repeating the simulations of the reference case three times. All the three simulations give the predicted wear volume of $5{,}861 \times 10^{-12}$ m^3. Based on this, we conclude that the DEM model of the pin-on-disc wear test can promote highly accurate and stable results.

5. Sensitivity analysis

The previous section verifies the accuracy and the stability of the pin-on-disc wear simulation model. Therefore, the sensitivities can be studied by analysing wear predictions for one revolution. This section first presents the sensitivity analysis based on material real properties. Besides, extended values of DEM parameters are investigated for reducing computational time.

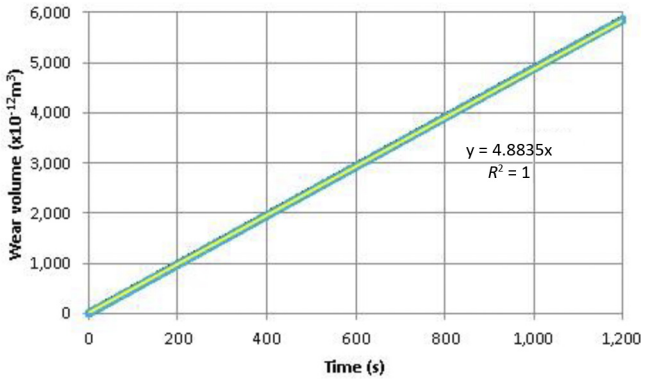

Figure 12.
Wear volume for 1,200 s (180 m) at the steady state

5.1 Simulation studies based on material real properties

Based on the determinations of DEM parameters in Section 3, nine variables from particle, disc, contact and simulation are identified. Table X lists the values for the nine variables to predict wear volumes.

For particle parameters, increasing radius or density can cause wear volume increases, which are shown in Figures 13-14. In comparison, increasing particle radius results in

Categories	DEM parameters	Values
Particle	Radius R_p [$\times 10^{-3}$ m]	1, 2, 3, 4
	Density ρ_p [kg/m^3]	4,750, 4,850, 4,950, 5,050
	Poisson's ratio ν_p	0.23, 0.24, 0.25, 0.26
	Shear modulus G_p [GPa]	60, 65, 70, 75
Disc	Rotating speed ω [rad/s]	2.27, 6.82, 11.36, 15.91
	Mesh size d_O [$\times 10^{-3}$m]	0.55, 1.1, 2.2, 4.4
Contact	Coefficient of restitution $e_{p,d}$	0.35, 0.40, 0.45, 0.50
Simulation	Indentation force F_p [N]	3, 5, 7, 9
	Time step Δt [$\times 10^{-6}$s]	1.0, 1.5, 2.0, 2.5

Table X. Values of DEM parameter for sensitivity analysis

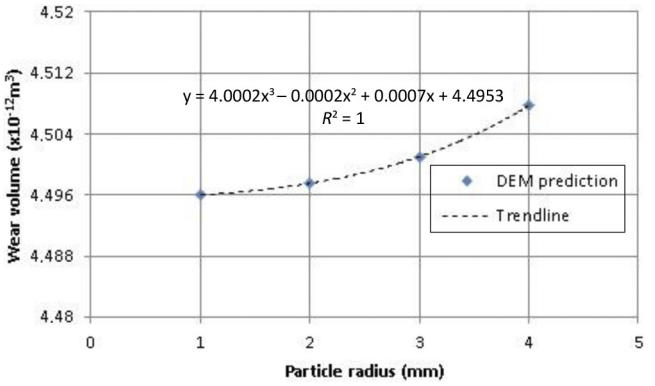

Figure 13. Wear as a function of particle radius

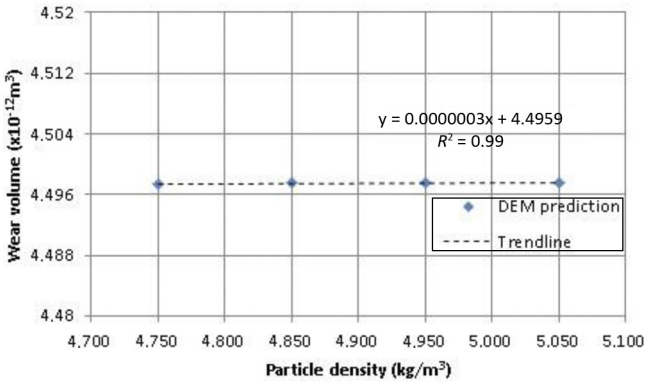

Figure 14. Wear as a function of particle density

notable wear volume increase. The reason for the increase is the extra gravitational forces that are applied to disk geometry because of the mass increase of the particle. Besides, the gravitational force depends on the particle radius to the power of three. Poisson's ratio and shear modulus show no influence, which give a volume of 4.50×10^{-12} m^3 as the theoretical calculation using equation (4).

For disc geometry parameters, it is examined that both rotating speed and mesh size have no influence on wear volume. This is because wear is a matter of sliding distance, instead of the individual parameter of rotating speed or time [equation (4)]. By comparing simulation predictions with experimental results, it demonstrates that wear is independent of the sliding speed at 0.10-0.35 m/s. For achieving a more uniform distribution compared to the results shown in Figure 6, the minimal size is restrained by the diameter of the indented area, which is $2\sqrt{R_p \delta_n}$ (Appendix 1). On the other hand, increasing the mesh size is preferable, as it can reduce computation time by decreasing the number of contacts. Referring to the mesh setting used for Figure 6, the maximum mesh size is set smaller than the particle radius R_p. Accordingly, the setting of mesh size is recommended at $2\sqrt{R_p \delta_n} < d_0 < R_p$.

For the contact parameter of the coefficient of restitution, all the DEM predictions give the wear volume of 4.50×10^{-12} m^3 that is equivalent to the theoretical calculation. This indicates that the coefficient of restitution does not influence the sliding wear at steady-state condition.

For the simulation parameters, the wear volumes with respect to indentation force are illustrated in Figure 15. It is observed that the wear increase is perfectly proportional to the indentation force, which is consistent with the theory by equation (4). The time step has no influence on the wear volumes for the tested values.

Table XI summarises the sensitivity analysis using the values determined by material real properties.

5.2 Simulation studies for reducing computational time

Section 5.1 presents the sensitivity analysis based on material real properties. However, to reduce computational time, many DEM simulations adopt lower shear moduli to increase time steps (Lommen *et al.*, 2014). Thus, lower shear moduli will be explored with regard to the reliability of wear prediction. In addition, higher time steps than previous values are applied to investigate the accuracy of the wear prediction.

Using the reference case values in Table IX, a series of lower particle shear moduli λG_p (λ = 1/10, 1/40, 1/70 and 1/100) are tested. Results demonstrate that the predicted wear volumes are not changed by lower moduli. However, to reach the applied indentation force,

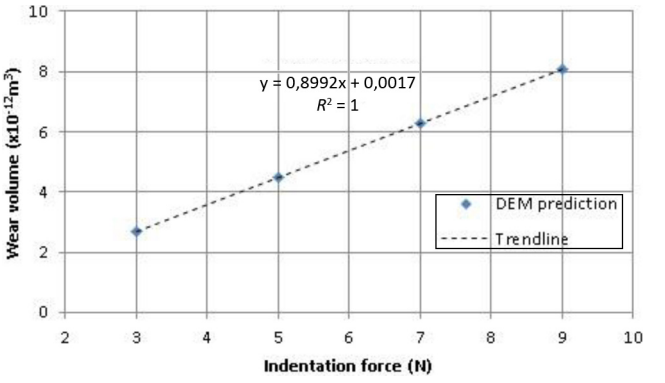

Figure 15.
Wear as a function of indentation force

using a lower shear modulus causes a higher normal overlap δ_n according to equation (3). This is illustrated in Figure 16, where a large increase of normal overlaps for lower particle shear moduli (λG_p) is observed in comparison to that from the realistic particle shear modulus ($1G_p$). Also, the indentation time is longer before arriving at a steady state with decreasing particle shear moduli. The influences on indentation depth and time might affect the flow behaviours of bulk-solids in direct contact with equipment. In addition, a change of particle shear modulus directly affects particle interaction and thus bulk behaviour. Therefore, to reduce computation time, it is not appropriate to use lower particle shear moduli for modelling the wear in bulk-solids-handling.

The wear predictions of the higher time steps [(160-240)% T_R, i.e. 3.0-4.5 $\times$ 10^{-6} s] are plotted in Figure 17. It shows that accurate prediction of 4.50 $\times$ 10^{-12} m^3 can still be achieved as time step is increased to 3.50 $\times$ 10^{-6}s, which is 187% T_R. Thus, the maximum time step for modelling sliding wear can be set by 187% T_R.

6. Conclusions

Using DEM, this research carried out a sensitivity analysis for modelling sliding wear by iron ore particles. Four conclusions are drawn as below:

Categories	DEM parameters	Influences
Particle	Radius R_p [$\times$ 10^{-3} m]	polynomial increase $y = 0.0002x^3 - 0.0002x^2 + 0.0007x + 4.4953$ $R^2 = 1$
	Density ρ_p [kg/m^3]	linear increase $y = 0.0000003x + 4.4959$ $R^2 = 0.99$
	Poisson's ratio ν_p	No influence
	Shear modulus G_p [GPa]	No influence
Disc	Rotating speed ω [rad/s]	No influence
	Mesh size d_0 [$\times$ 10^{-3}]	No influence
Contact	Coefficient of restitution $e_{p,d}$	No influence
Simulation	Indentation force F_p [N]	Linear increase $y = 0.8992x + 0.0017$ $R^2 = 1$
	Time step Δt [$\times 10^{-6}$s]	No influence

Table XI. Results of sensitivity studies based on material real properties

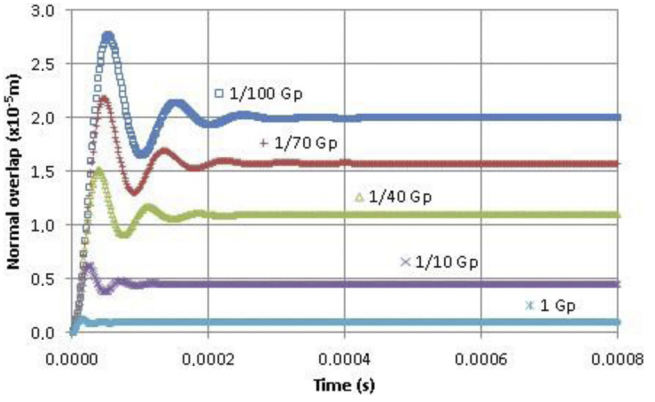

Figure 16. Normal overlaps as functions of particle shear moduli

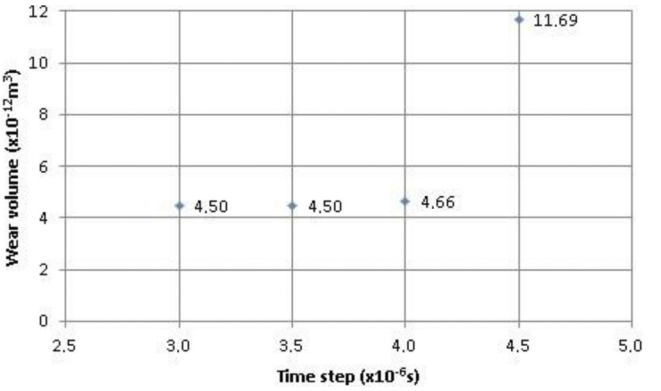

Figure 17.
Wear volume with respect to higher time steps [(160-240)% T_R]

(1) Numerical error occurs as a particle passes a joint side of meshes. However, this influence on total wear volume is negligible. By comparing DEM predictions with the theoretical calculations, it demonstrates that the predictions of sliding wear volume are accurate and stable.

(2) For the steady-state wear, increasing particle density or radius results in higher wear. By contrast, particle Poisson's ratio, particle shear modulus, geometry mesh size, rotating speed, coefficient of restitution and time step have no impact on wear. As expected, increasing the indentation force results in a proportional wear volume increase.

(3) For maintaining wear characteristic and reducing simulation time, the geometry mesh size is recommended at $2\sqrt{R_p \delta_n} < d_0 < R_p$. To further reduce simulation time, it is inappropriate using a lower particle shear modulus. However, the maximum time step can be increased to 187% T_R without compromising simulation accuracy.

(4) This research enables the selections of adequate values to predict sliding wear in iron ore-handling industry. Nevertheless, to apply this simulation model to predict realistic wear volumes, the coefficient of sliding wear α_s is required to be experimentally determined by taking into account the non-spherical shapes of iron ore particles.

References

ANSYS (2016), *ANSYS® Workbench 16.2: Mesh-Meshing*, ANSYS Inc., Pennsylvania.

Archard, J.F. (1953), "Contact and rubbing of flat surfaces", *Journal of Applied Physics*, Vol. 24 No. 8, pp. 981-988.

ASTM (2000), "Standard test method for wear testing with a pin-on-disk apparatus", *Annual Book of ASTM Standards, G-99-95a*, ASTM, Philadelphia, pp. 1-5.

Barrios, G.K., de Carvalho, R.M., Kwade, A. and Tavares, L.M. (2013), "Contact parameter estimation for DEM simulation of iron ore pellet handling", *Powder Technology*, Vol. 248, pp. 84-93.

Bingley, M.S. and Schnee, S. (2005), "A study of the mechanisms of abrasive wear for ductile metals under wet and dry three-body conditions", *Wear*, Vol. 258 Nos 1/4, pp. 50-61.

Brown, N.J., Chen, J.F. and Ooi, J.Y. (2014), "A bond model for DEM simulation of cementitious materials and deformable structures", *Granular Matter*, Vol. 16 No. 3, pp. 299-311.

Cleary, P.W. (1998), "Predicting charge motion, power draw, segregation and wear in ball mills using discrete element methods", *Minerals Engineering*, Vol. 11 No. 11, pp. 1061-1080.

Cleary, P.W., Owen, P., Hoyer, D.I. and Marshall, S. (2010), "Prediction of mill liner shape evolution and changing operational performance during the liner life cycle: Case study of a Hicom mill", *International Journal for Numerical Methods in Engineering*, Vol. 81 No. 9, pp. 1157-1179.

Cleary, P.W., Sinnott, M. and Morrison, R. (2006), "Analysis of stirred mill performance using DEM simulation: Part 2 – Coherent flow structures, liner stress and wear, mixing and transport", *Minerals Engineering*, Vol. 19 No. 15, pp. 1551-1572.

Cleary, P.W., Sinnott, M.D. and Morrison, R.D. (2009), "Separation performance of double deck banana screens – part 2: quantitative predictions", *Minerals Engineering*, Vol. 22 No. 14, pp. 1230-1244.

Cundall, P.A. and Strack, O.D. (1979), "A discrete numerical model for granular assemblies", *Geotechnique*, Vol. 29 No. 1, pp. 47-65.

DEM Solutions. (2016), *EDEM® 2.7*, DEM Solutions, Edinburgh.

George, E.D.J. (1961), *Mechanical Metallurgy*, McGraw Hill Book Company, New York, NY, Toronto, London.

Hilgraf, P. (2007), "Wear in bulk materials handling", *Bulk Solids Handling*, Vol. 27 No. 7, pp. 464-477.

Jafari, A. and Nezhad, V.S. (2016), "Employing DEM to study the impact of different parameters on the screening efficiency and mesh wear", *Powder Technology*, Vol. 297, pp. 126-143.

Jourani, A. and Bouvier, S. (2015), "Friction and wear mechanisms of 316L stainless steel in dry sliding contact: effect of abrasive particle size", *Tribology Transactions*, Vol. 58 No. 1, pp. 131-139.

Kalala, J.T. and Moys, M.H. (2004), "Discrete element method modelling of liner wear in dry ball milling", *Journal of the South African Institute of Mining and Metallurgy*, Vol. 104 No. 10, pp. 597-602.

Kano, J., Kasai, E., Saito, F. and Kawaguchi, T. (2005), "Numerical simulation model for granulation kinetics of iron ores", *ISIJ International*, Vol. 45 No. 4, pp. 500-505.

Keppler, I., Varga, A., Szabo, I., Katai, L. and Fenyvesi, L. (2016a), "Particle motion around open mixing screws: optimal screw angular velocity", *Engineering Computations*, Vol. 33 No. 3, pp. 896-906.

Keppler, I., Safranyik, F. and Oldal, I. (2016b), "Shear test as calibration experiment for DEM simulations: a sensitivity study", *Engineering Computations*, Vol. 33 No. 3, pp. 742-758.

Lommen, S., Schott, D. and Lodewijks, G. (2014), "DEM speedup: Stiffness effects on behavior of bulk material", *Particuology*, Vol. 12 No. 1, pp. 107-112.

Lommen, S.W. (2016), "Virtual prototyping of grabs: co-simulation of discrete element method and rigid body models", The doctoral thesis, Delft University of Technology, Delft.

Minoru, A. and Yasuo, O. (1983), "Determination of young's modulus and Poisson ratio of lump ores", *The Iron and Steel Institute of Japan*, Vol. 69 No. 7, pp. 739-745.

Mishra, B.K. and Rajamani, R.K. (1992), "The discrete element method for the simulation of ball mills", *Applied Mathematical Modelling*, Vol. 16 No. 11, pp. 598-604.

Miszewski, A., Lommen, S.W., Schott, D.L. and Lodewijks, G. (2012), "Effect of moisture content on the angle of repose of iron ore", 7th International Conference for Conveying and Handling of Particulate Solids, *Friedrichshafen*.

Popov, V.L. (2010), *Contact Mechanics and Friction: Physical Principles and Applications*, Springer, Heidelberg, Dordrecht, London, New York, NY.

Powell, M.S., Weerasekara, N.S., Cole, S., LaRoche, R.D. and Favier, J. (2011), "DEM modelling of liner evolution and its influence on grinding rate in ball mills", *Minerals Engineering*, Vol. 24 No. 3, pp. 341-351.

Rezaeizadeh, M., Fooladi, M., Powell, M.S., Mansouri, S.H. and Weerasekara, N.S. (2010), "A new predictive model of lifter bar wear in mills", *Minerals Engineering*, Vol. 23 No. 15, pp. 1174-1181.

Roberts, A.W. (2003), "Chute performance and design for rapid flow conditions", *Chemical Engineering and Technology*, Vol. 26 No. 2, pp. 163-170.

Roberts, A.W. and Wiche, S.J. (1993), "Prediction of lining wear life of bins and chutes in bulk solids handling operations", *Tribology International*, Vol. 26 No. 5, pp. 345-351.

Sato, A., Kano, J. and Saito, F. (2010), "Analysis of abrasion mechanism of grinding media in a planetary mill with DEM simulation", *Advanced Powder Technology*, Vol. 21 No. 2, pp. 212-216.

Tan, Y., Zhang, H., Yang, D., Jiang, S., Song, J. and Sheng, Y. (2012), "Numerical simulation of concrete pumping process and investigation of wear mechanism of the piping wall", Tribology International, Vol. 46 No. 1, pp. 137-144.

Taylor, D.J.C., Page, D.C. and Geldenhuys, P. (1988), "Iron and steel in South Africa", *Journal of the South African Institute of Mining and Metallurgy*, Vol. 88 No. 3, pp. 73-95.

Xie, L., Zhong, W., Zhang, H., Yu, A., Qian, Y. and Situ, Y. (2016), "Wear process during granular flow transportation in conveyor transfer", *Powder Technology*, Vol. 288, pp. 65-75.

Appendix 1

The sliding wear from a meshed geometry surface for a distance l is given by Archard (1953):

$$W_V = \alpha_s \cdot F_n \cdot l \tag{A.1}$$

According to the sphere indentation against a flat surface (Figure 5), for the equal wear distance l and the same conditions, the wear volume is:

$$W_V = \phi \cdot A_0 \cdot l \tag{A.2}$$

Combining equations (A.1) and (A.2), it gives:

$$\alpha_s F_n = \phi A_0 \tag{A.3}$$

Accordingly:

$$\alpha_s = \frac{\phi A_0}{F_n} \tag{A.4}$$

in which ϕ is the fraction of material removal from the indented groove; A_0 is the cross-sectional area of sphere indentation; and F_n is the reaction force. Corresponding to Figure 5, A_0 is expressed as:

$$A_0 = \frac{\theta R_p^2}{2} - a\left(R_p - \delta_n\right) \tag{A.5}$$

where θ is the indention angle and a is the radius of contact area, which is given by Popov (2010):

$$a = \sqrt{R_p \delta_n} \tag{A.6}$$

θ can be obtained from:

$$\sin\frac{\theta}{2} = \frac{a}{R_p} \tag{A.7}$$

Substituting a by using equations (A.6) and (A.7) gives:

$$\theta = 2arc\sin\left(\frac{\delta_n}{R_p}\right)^{1/2} \tag{A.8}$$

Using equations (A.6) and (A.8), A_O becomes:

$$A_0 = \left[arc\sin\left(\frac{\delta_n}{R_p}\right)^{1/2} - \left(\frac{\delta_n}{R_p}\right)^{1/2} + \left(\frac{\delta_n}{R_p}\right)^{3/2}\right]R_p^2 \tag{A.9}$$

F_n can be expressed by Popov (2010):

$$F_n = \frac{4}{3}E^* R_p^{1/2}\delta_n^{3/2} = \frac{4}{3}E^*\left(\frac{\delta_n}{R_p}\right)^{3/2}R_p^2 \tag{A.10}$$

The coefficient of wear α_s is then obtained by substituting equations (A.9) and (A.10) into equation (A.4):

$$\alpha_s = \frac{3\phi\left[arc\sin\left(\frac{\delta_n}{R_p}\right)^{1/2} - \left(\frac{\delta_n}{R_p}\right)^{1/2} + \left(\frac{\delta_n}{R_p}\right)^{3/2}\right]}{4E^*\left(\frac{\delta_n}{R_p}\right)^{3/2}} \tag{A.11}$$

Appendix 2

To determine $\frac{\delta_n}{R_p}$ in equation (A.11), the correlation between hardness and yield stress is applied (Popov, 2010):

$$H_e \approx 3\sigma_c \tag{B.1}$$

where σ_c is yield stress, which can be equated to the maximum pressure stress P_m subjected to a spherical particle indentation (Hilgraf, 2007):

$$\sigma_c \approx P_m \tag{B.2}$$

For a rigid spherical particle indenting against an elastic half-space, the maximum pressure stress P_m is given by Popov (2010):

$$P_m = \frac{2}{\pi}E^*\left(\frac{\delta_n}{R_p}\right)^{1/2} \tag{B.3}$$

Substituting σ_c in equation (B.1) by using equation (B.3), gives:

$$\frac{\delta_n}{R_p} = \left(\frac{\pi H_e}{6E^*}\right)^2 \tag{B.4}$$

The hardness of mild steel is experimentally measured at H_e = 1.38 GPa. The equivalent Young's modulus E^* = 96.74GPa using Table II. Eventually, it calculates $\frac{\delta_n}{R_p} = 5.58 \times 10^{-5}$.

Appendix 3

Assuming A_r is the real loss from the area of the displaced groove A_O, then the fraction ϕ is expressed by:

$$\phi = \frac{A_r}{A_0} \tag{C.1}$$

A_r can be measured from a wear profile for one revolution of a pin-on-disc test. However, A_r is difficult to measure with respect to single revolution. Therefore, a number of revolutions (N) are proceeded to obtain total loss A_N from the displaced groove. Thus, the area loss A_r for one revolution is evaluated by:

$$A_r = \frac{A_N}{N} \tag{C.2}$$

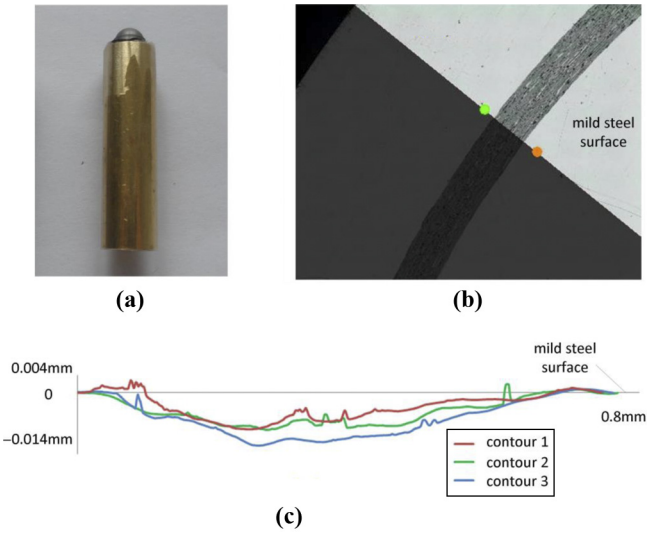

Figure A1.
Determination of the coefficient of fraction

Notes: (a) a pin with a spherical head of iron ore particle; (b) measuring an area of cross-section; (c) three wear contours based on three measurements

To obtain A_N, a pin with a spherical head was fabricated from a natural Sishen iron ore particle, which is shown in Figure A1(a). Figure A1(b) illustrates the approach to measure a cross section from the wear path after N revolutions of a pin-on-disc test. Figure A1(c) displays the three wear contours from three measurements. A_N is obtained by using the net area below the referential mild steel surface.

In the pin-on-disc test of using the spherical head of Sishen iron ore particle R_p = 3 mm, revolutions N = 1,302.5 which corresponding to l = 180 m, the mean value of the net area A_N for the three wear contours is 4.13×10^{-9} m^2. Using equation (C.2), the average loss per revolution $A_r = 3.16 \times 10^{-12}$ m^2. In combination with $A_0 = 3.74 \times 10^{-12}$ m^2 from equation (A.9), the coefficient of fraction [equation (C.1)] is calculated as $\phi = 0.84$.

About the authors

Guangming Chen received his bachelor and master degrees from Jilin University (during 2005 to 20012), China. His research background is mechanical design on wear reduction. During the research for his master degree, he studied wear behaviours of several bionic structures using discrete element method (DEM) in the Key Laboratory of Bionic Engineering (Jilin University), Ministry of Education, China. In 2012, he obtained the TU Delft/CSC Scholarship and started his doctoral research on the topic "Wear Reduction of Transportation Equipment using DEM and Bionic Design" at Delft University of Technology, The Netherlands. Guangming Chen is the corresponding author and can be contacted at: G.Chen-1@tudelft.nl

Ms. Dingena L. Schott (Associate Professor) has a background in Mechanical Engineering. She obtained her MSc in 1999 in the field of Dredging Engineering. In her years as a PhD student, she focused on the field of bulk-solids-handling with her thesis on "Large-scale Homogenization of Bulk Materials in Mammoth Silos". She obtained her PhD in 2004. After two years of experience with organization management, she was appointed Assistant Professor at Delft University of Technology (Department of Marine and Transport technology) in 2006 and has carried out several projects with industry.

Prof Gabriel Lodewijks studied Mechanical Engineering at Twente University and Delft University of Technology, The Netherlands. He obtained a master's degree in 1992 and a PhD on the dynamics of belt systems in 1996. He is President of Conveyor Experts BV, which he established in 1999. In 2000, he was appointed Professor of the department Transport Engineering and Logistics at the Faculty of Mechanical, Maritime and Materials Engineering. From 2002, he was appointed as Chairman of the department. His main interests are in belt conveyor technology, automation of transport systems, material engineering and dynamics.